SUPPLEMENTAL EXPERIMENTAL PROCEDURES

Materials and reagents

Lipofectamine 2000 and RNAi-Max were purchased from ThermoFisher (Carlsbad, CA). SiRNAs to *FOXM1* (Cat#1 109415, Cat#2 6312) and *MAT1A* (Cat# 4392420, Cat#4392421) were purchased from ThermoFisher. FOXM1 overexpressing and empty vectors were purchased from GeneCopoeia (Rockville, MD). FDI-6 (NCGC 00099374) was purchased from Axon (Reston, VA). T0 (Cas No.293754-55-9) was purchased from Sigma (St. Louis, MO).

Source of normal liver, human HCC and CCA with adjacent non-tumorous tissues, primary biliary cholangitis (PBC) and primary sclerosing cholangitis (PSC)

All human materials were obtained with patients' informed content. Seven human CCA and five human HCC specimens and adjacent benign tissues were obtained from patients that underwent surgical resection at the Cedars-Sinai Medical Center, Los Angeles, CA. One hundred and forty three human HCC and adjacent non-tumorous tissues were obtained from patients undergoing surgical liver resection from 2013 to 2017, five PBC and three PSC human liver specimens obtained from liver biopsy from 2014-2019, and five normal liver tissues obtained from surgical resection for patients suffering from intrahepatic ductal stones from 2018-2019 were obtained from the department of Pathology at the Xiangya Hospital Central South University, Changsha, Hunan province, China and were stored in liquid nitrogen in the institutional biobank.

Establishment of malignant HCC cell line from Mat1a knockout (KO) mice

Fresh HCC tissue from 15-month old male *Mat1a* KO mouse was rinsed with DMEM

medium (Corning cellgro, Tewksbury MA) supplemented with Penicillin-Streptomycin solution (Hyclone, South Logan, UT), and minced into 1-mm^3 pieces. After digestion with collagenase from Clostridium histolyticum (Sigma) for five minutes at 37°C three times, disaggregated cell suspension was filtered by a 40 μm cell strainer (ThermoFisher Scientific). After lysis of red blood cells by Ammonium-Chloride-Potassium (ACK) lysis buffer (ThermoFisher), cells were washed with DMEM medium twice. The cells were then resuspended in DMEM supplemented with 10% fetal bovine serum (FBS) (ThermoFisher), and then seeded onto 6-well culture plates coated with 0.1% type I collagen (Sigma). Cells were incubated at 37°C at 95% air and 5% CO_2 for two days. The culture medium was then changed twice a week and cells were sub-passaged when they reached 75-85% confluency.

Human hepatocytes, cell lines and treatments

Primary human hepatocytes were from ThermoFisher (Lot# HU8250, viabilities >80%). The cells were centrifuged at 2000rpm (2 minutes) to eliminate the cell freezing medium. The cell pellets were resuspended with DMEM containing 10% FBS and were seeded in 100 mm BioMatrix dishes at a cell density of $5X10^6$ cells/dish. After 6 hours attachment period, the cells were transfected for 24hrs.

MzChA-1 (human biliary adenocarcinoma), HepG2 (human hepatoblastoma), Hep3B (human hepatocellular carcinoma), H69 (human normal biliary epithelial cells),[16] SAMe-D (HCC cell line from *Mat1a* KO mouse),[26] and OKER cells (HCC cell line from glycine N-methyltransferase (*Gnmt*) KO mice)[27] were cultured in DMEM supplemented with 10% FBS, 100 U/mL penicillin, 0.1 mg/mL streptomycin, and 2 mmol/L L-glutamine. To examine the crosstalk between MAT1A and FOXM1/NF-κB, $1x10^5$ HepG2, MzChA-1, Hep3B, H69, normal human hepatocytes, SAMe-D, MATα1-D, or OKER cells per well

of 6-well plates were transfected with vectors overexpressing FOXM1, MAT1A (wild type and catalytic mutant that cannot oligomerize), p65, or empty vectors for 24 hours using Lipofectamine 2000 according to the manufacturer's protocol. For gene knockdown studies, 10 nM siRNA against *FOXM1*, *MAT1A*, and equivalent scramble control were delivered into HepG2, MzChA-1, Hep3B, SAMe-D, MATα1-D, or OKER cells for 24 hours by Lipofectamine RNAiMAX following the manufacturer's protocol. To inhibit FOXM1, cells were treated with T0 (5-30 μM) or FDI-6 (5-30 μM) for 24-48h.

Xenograft model and treatment with T0 or FDI-6

In one experiment, 4-week-old male BALB/c nude mice (weighing 16-18g) were purchased from Shanghai SLAC Laboratory Animal Co., Ltd. (Shanghai, China). They were injected with HepG2 cells ($5x10^6$) in 100 μl saline subcutaneously into the right flank. When the tumor size reached $80mm^3$, mice were divided into two groups (8 mice per group), one received T0 (25 mg/kg/d) via intraperitoneal injection every two days and the other received vehicle. Xenograft tumor size was measured by caliper, with the tumor volume calculated according to the formula: π/6 (length x width x height). Animals were sacrificed on day 28. Tumor tissues were used for RNA and protein analysis and some were fixed in 4% formalin for histology and immunohistochemistry (IHC). All procedure protocols and the care of the animals were reviewed and approved by the Institutional Animal Care and Use Committee of University of South China (Hengyang, China).

In a separate experiment, 4-week old male nude mice were purchased from Jackson Labs (Bar Harbor, ME). They were injected with MzChA-1 cells ($5x10^6$) in 100 μl saline subcutaneously into the right and left flanks. Treatment with either T0 or FDI-6 (both at 25 mg/kg/d in 50μl volume) via direct intratumoral injection was started when tumors

reached 80mm^3. Each mouse received one type of treatment on tumors on one flank and DMSO injection on the contralateral tumor. Tumor size was measured as above, and experiment was terminated on day 30 after initial injection.

Syngeneic tumorigenesis and treatment with FDI-6

Three-month-old male C57BL/6J mice were injected with OKER or MATα1-D cells ($5x10^6$) in 100µl phosphate buffered saline subcutaneously into the flanks. From day seven after injection, mice were divided into four treatment groups (n=8 per group) that received MATα1-D+DMSO, MATα1-D+FDI-6, OKER+DMSO, OKER+FDI-6. Tumor size was measured as above. FDI-6 treatment groups received FDI-6 (25 mg/kg/d in 50µl volume) via direct intratumoral injection every day for four days and control groups received 50µl DMSO. Animals were sacrificed on day 11. Tumor tissues were used for RNA and protein analysis and some were fixed in 4% formalin for histology and IHC.

Promoter constructs and luciferase assay

The human *MAT1A* promoter was described previously.[29] Subcloning of *MAT1A* promoter into pGL3 vector was performed by forward primers: 5'-AATGTGTGCCAGAAAAAATTTTTCC-3' (-1087 to -1111 bp relative to transcription start site), 5'-TACATGAACTAAAGATATAATCCTG-3' (-814 to -839 bp relative to transcription start site), 5'-GGGAAACTGGACTTTGATAATTTC-3' (-681 to -705 relative to transcription start site), and reverse primers 5'-CTGCTTGCCACAGCTTGCTCCTG-3' (+8 to +30). The constructs that contain the 5'- flanking sequences (-1111 to +30, -839 to +30 and -705 to +30) were used in the transfection assay. Mutagenesis of the *MAT1A* promoter FOX binding sites were performed as follows: 5'-TGTTTA-3' (-811 to -816) was changed to 5'-TGTGTA-3' using forward primer 5'-AAGATATAATCCTGTGTACTACTTTTTTTGG-3' (-798 to -828 bp relative to

transcription start site); 5'-TGTTTA-3' (-754 to -759) was changed to 5'-TGTGTA-3' using forward primer 5'-ATGTGAACACGATGTGTATTACATGTATAG-3', (-742 to -771), and 5'-TGTTTA-3' was changed to 5'-TGTGTA-3' (-721 to -726) using forward primer 5'-GAATATGTAGATGTTTATAATCCGGAAGC-3' (-702 to -737) with QuikChange multisite-Directed mutagenesis kit (#200515-5) from Agilent Technologies (Carpinteria, CA). The mutant strand synthesis reaction consisted of an initial denaturation at 95°C for 30 seconds followed by 16 cycles at 95°C for 30 seconds, annealing at 55°C for one minute and extension at 68°C for one minute/kb of plasmid length using the PfuUltra HF DNA polymerase. *Dpn*I digestion of the amplified PCR products and transformation of XL10-gold ultracompetent cells were done in accordance with their suggested protocol (Agilent Technologies).

The human 1.3kb *FOXM1* promoter was purchased from Genecopoeia (NM_001243088). Mutagenesis of the *FOXM1* promoter FOX binding sites were performed as follows: 5'-TGTTTG-3' (-1022 to -1027) was changed to 5'-GGTTTG-3' using forward primer 5'- GCAATAATTCAACATTGGTTTGTTTTGGAGAC-3' (-1012 to -1043 bp relative to transcription start site), and 5'-TGTTTA-3' (-732 to -737) was changed to 5'-TGTTGA-3' using forward primer 5'-GCCCACATTTGTTGATTTGATTAA AATGTC-3', (-717 to -751), with QuikChange multisite-Directed mutagenesis kit. Constructs containing multimerized enhancer elements of FOX (5'-TTGTTTATG-3')x8 and its mutant (5'-TTGTCTATG-3')x8 were cloned into a pLuc-MCS Cis-Reporter Cloning Plasmid from Agilent Technologies.

Various promoter constructs and their empty vectors/SV40, and FOX x8 enhancer elements and pLuc-MCS were co-transfected into HepG2 and MzChA-1 cells and NF-κBx5 construct and pLuc-MCS were transfected into HepG2, normal human

hepatocytes and SAMe-D cells with Lipofectamine 2000 following the manufacturer's instructions. Luciferase assays were performed 24 hours later using the Dual Luciferase Reporter Assay System (Promega, Madison, WI) as directed by the manufacturer suggested protocol.

Histology and immunohistochemistry (IHC)

Formalin-fixed liver tissues embedded in paraffin were cut and stained with hematoxylin and eosin (H&E) for routine histology. IHC staining of FOXM1, MATα1, p65, p50 and IgG was performed with kits from Dako (Carpinteria, CA) or Abcam (Burlingame, CA) according to the manufacturer's method. Control with normal mouse IgG showed no staining (data not show).

RNA isolation and gene expression analysis

Total RNA was isolated by using the Quick-RNA miniPrep kit (Zymo Research, Irvine, CA) or TRIzol reagent (ThermoFisher) from cell lines, murine, HCC and CCA tissues. Gene expression was assessed using real-time PCR. Total RNA was subjected to reverse transcription (RT) by using M-MLV Reverse transcriptase (Lucigen, Middleton, WI). TaqMan probes for human and mouse *FOXM1*, *MAT1A*, *NF-κB1, RELA,* and matrix metalloproteinase-7 (*MMP-7*) were purchased from ThermoFisher and the Universal PCR Master Mix was purchased from Bio-Rad (Hercules, CA). Hypoxanthine phosphoribosyltransferase 1 was used as a housekeeping gene. The thermal profile consisted of an initial denaturation at 95°C for 3 minutes followed by 40 cycles at 95°C for 3 seconds and at 60°C for 30 seconds. The cycle threshold (Ct value) of the target genes was normalized to that of the housekeeping gene to obtain the delta Ct (ΔCt). The ΔCt was used to find the relative expression of target genes according to the

formula: relative expression= $2^{-\Delta\Delta Ct}$, where $\Delta\Delta Ct$= ΔCt of target genes in experimental condition – ΔCt of target gene under control condition.

Chromatin immunoprecipitation (ChIP) and sequential-ChIP (Seq-ChIP) assay

ChIP was done to examine changes in protein binding to the FOX binding region of the human *MAT1A* and *FOXM1* promoters using the manufacturer's suggested protocol from the EpiTect ChIP OneDay kit (Qiagen, Germantown, MD). Briefly, DNA immunoprecipitated by FOXM1 antibody was processed for a second round of immunoprecipitation using anti-MATα1, anti-p65 or anti-p50 antibodies. The purified DNA was detected by PCR analysis. PCR primers for promoter regions containing FOX binding sites were 1) *MAT1A* - forward 5'- TTGTTCCTTGGGTCTGAGGATGCAG-3' (-872 to -897) and reverse 5'- CAAAGTCCAGTTTCCCAAAGCTTCCG -3' (-687 to -714) (GenBank® accession no. NM-000429), and 2) *FOXM1* - forward 5'- CATTTGTTT GTTTTGGAGACGGTGTC-3' (–1006 to -1031) and reverse 5'- GGAAGAGGGGCACAGACATTTTAATC-3' (–703 to -728) (GenBank® accession no. NM-001243088). All PCR products were run on 2% agarose gels. The PCR conditions consisted of an initial denaturation at 94°C for three minutes followed by 25 cycles at 94°C for 30 seconds, annealing and extension at 67°C for 90 seconds using the Advantage GC 2 PCR kit (Clontech, MountainView, CA), in accordance to their suggested protocol.

Ingenuity pathway analysis (IPA)

IPA investigated the molecular pathways involved in HCC and CCA by comparing SAGE library with an adjacent non-cancerous liver SAGE library using the website: www.ingenuity.com. All reliable transcripts statistically dysregulated in HCC and CCA were investigated and annotated with biological processes, protein-protein interactions,

and gene regulatory networks, using a reference-based data file with statistical significance. All identified pathways were screened individually.

SUPPLEMENTAL FIGURE LEGENDS

Figure S1. Inverse relationship between *MAT1A* and *FOXM1* mRNA levels in HCC and CCA datasets. All raw *FOXM1* and *MAT1A* mRNA levels in HCC (**A**) and CCA (**B**) were downloaded from the GEO database. Number in the parentheses next to the GEO database is the number of cases with HCC or CCA as compared to adjacent or normal liver tissues. Results depict Pearson correlation analysis of the raw data.

Figure S2. Relationship between *MAT1A* and *NF-κB1* or *RELA*, *FOXM1* and *NF-κB1* mRNA levels in HCC from the GEO database. **A-B**) Pearson correlation analysis shows inverse relationship between *MAT1A* and *NF-κB1* mRNA levels (**A**), and *MAT1A* and *RELA* mRNA levels (**B**). **C**) Pearson correlation analysis shows positive correlation between *FOXM1* and *NF-κB1* mRNA levels. Number in the parentheses next to the GEO database is the number of cases with HCC as compared to adjacent or normal liver tissues.

Figure S3. Protein expression of MATα1, FOXM1, p50, and p65 from normal liver, primary biliary cholangitis (PBC) and primary sclerosing cholangitis (PSC). **A**) Representative H&E and immunohistochemistry (IHC) staining of MATα1, FOXM1, p50, and p65 from normal liver, PBC and PSC are shown (lower power images are at 200X, higher power of the boxed areas is at 400X). Red arrows point to presence or absence of these proteins in the nuclei.

Figure S4. FOXM1 does not regulate NF-kB expression in MATα1-D cells. **A-B**) Western blotting for MATα1, FOXM1, p50, and p65 at baseline and after FOXM1 siRNA (**A**) and overexpression (**B**) in MATα1-D cells. **C**) Comparison of cell growth between SAMe-D and MATα1-D cells. *$p < 0.05$ vs. SAMe-D. **D**) Effects of FDI-6 or FOXM1 siRNA treatment on the *NF-κB* promoter activity in MATα1-D cells. Results are mean ± SEM from three experiments done in duplicates. **E)** WT mice were injected with MATα1-

D cells ($5x10^5$) on each flank and FDI-6 treatment (5μM based on tumor volume) was begun on day 7 as described in Methods. Results are expressed as mean of control ± SEM from eight tumors per group. *p < 0.05 vs. DMSO. **F)** Representative tumor pictures in DMSO (left) and FDI-6 treatment (right) groups at day 11.

Figure S5. FOXM1 regulates *MAT1A* promoter activity at the FOX binding sites in MzChA-1 cells. **A**) Nucleotide sequence of the 5'-flanking region of the human *MAT1A* promoter. Sequence is numbered relative to the transcriptional start site nearest the TATA box. The putative regulatory elements are indicated underneath the sequences. Three FOX binding sites are indicated in red. **B**) Effects of T0 and FDI-6 on the activity of *MAT1A* promoter (-839/30) in MzChA-1 cells. Results are expressed as mean % of control ± SEM from three experiments done in triplicates. *p < 0.05 vs. DMSO. **C**) Activities of the wild-type and FOX binding site mutants of the *MAT1A* promoter after FOXM1 OV or si treatment for 24 hours in MzChA-1 cells. Results are expressed as mean % of EV or SC ± SEM from three experiments done in triplicates. *p < 0.05 vs. EV or SC.

Figure S6. MATα1 is a co-repressor at the FOX binding sites of the *FOXM1* promoter. **A**) Nucleotide sequence of the 5'-flanking region of the human *FOXM1* promoter. Sequence is numbered relative to the transcriptional start site. FOX binding sites are in red, while NF-kB sites are in green. **B**) Effects of MAT1A OV or si on wild type (WT) or mutant (MU) 8x*FOXM1* promoter activity in MzChA-1 cells. Results are expressed as mean % of EV or SC ± SEM from three experiments done in triplicates. *p < 0.05 vs. EV or SC of WT construct.

Figure S7. Protein and mRNA expression of MATα1, FOXM1, p50 and p65 in tumorous and adjacent tissues from *Mat1a-/-* mice. **A**) Representative IHC of MATα1, FOXM1, p50, and p65 in 15-month old *Mat1a*-/- and WT male mice. Top row = WT livers (x200); middle (x200) and bottom (x400) rows = HCC from *Mat1a*-/- mice

livers. Arrow points to the magnification position. **B-D**) Representative gross features (**B**), *Mat1a* (**C**), and *Foxm1* (**D**) mRNA level of WT liver tissues, *Mat1a*-/- adjacent and tumorous tissues. **E**) Western blotting of MATα1, FOXM1, p50, and p65 in WT liver tissues, *Mat1a*-/- adjacent and tumorous tissues. **F**) Densitometric values of **E**). *p < 0.05 vs. WT liver tissues. #p < 0.05 vs. *Mat1a*-/- adjacent tissues.

FOXM1 (**E**) and *MAT1A* (**F**) mRNA levels.

Figure S8. MAT1A and FOXM1/NF-kB reciprocal interplay does not occur in normal human hepatocytes or biliary epithelial cells. Western blotting for MATα1, FOXM1, p50, and p65 at baseline and after MAT1A or FOXM1 overexpression for 24 hours in normal human hepatocytes and H69 cells (normal human biliary epithelial cells). *p<0.05 vs. EV.

Figure S9. Effects of MAT1A and FOXM1 on migration in Hep3B cells. Effects of varying MAT1A and FOXM1 expressions on Hep3B cell migration was examined as described in Experimental Procedures. Quantitative values are summarized in the graph below. Results are expressed as mean % of EV+EV or SC+SC ± SEM from three experiments done in duplicates. *p < 0.05 vs. EV+EV or SC+SC; #p < 0.05 vs. FOXM1 OV or siRNA; †p < 0.05 vs. MAT1A OV or siRNA.

Figure S10. Effect of T0 and FDI-6 on cell growth, and protein levels of MATα1, FOXM1, p65, and p50 in MzChA-1 cells. **A**) Dose-response curve of FDI-6 treatment for 24 hours on cell growth in MzChA-1 cells. Results are from three experiments expressed as percent of 0 ± SEM. *p < 0.05 vs. DMSO; #p<0.05 vs. FDI-6 (10uM). **B-C**) Protein expression of MATα1, FOXM1, p50, and p65 after T0 (**B**) and FDI-6 (**C**) treatment in MzChA-1 cells. Numbers below the blots are densitometric values expressed as % of DMSO control ± SEM from three independent experiments. *p < 0.05 vs. DMSO.

Figure S11. Effects of T0 and FDI-6 on expression of MATα1, FOXM1, p50 and p65, and tumor growth. **A**) Pictures of liver xenograft tumors at day 28 after injection of MzChA-1 cells in DMSO and T0 or FDI-6 treatment groups. **B**) Average tumor volume of the three groups are shown over time. Treatments were started on day 9. **C**) H&E from the tumors show necrosis in the T0 and FDI-6 treated groups (X100). **D**) Representative IHC pictures are shown from n = 8 each (X200) for expression of MATα1, FOXM1, p50 and p65.

Figure S12. Ingenuity pathway analysis. Ingenuity pathway analysis was performed as described in Experimental Procedures on the MAT1A, FOXM1, and NF-κB data in CCA (**A**) and HCC (**B**). Representative canonical pathways are associated with FOXM1, MATα1, NF-κB and other related genes (including the transcription regulator, enzymes and other molecules) of HCC or CCA. Functional relationships of these genes are depicted using straight lines with arrows. Solid lines show direct regulation while dotted lines depict indirect interactions.

Figure S13. Interplay between MAT1A and FOXM1/NF-κB in liver cancer. MATα1 and NF-κB (p65/p50) interact with FOXM1 at the FOX elements of *MAT1A* and *FOXM1* promoters. While NF-κB co-activate the FOX element, MATα1 co-repress. Interestingly, the FOX elements in the *MAT1A* promoter function as repressors but the FOX element in the *FOXM1* promoter is an enhancer. This explains how MAT1A and FOXM1 exert reciprocal negative regulation against each other. Similarly, FOXM1 and MATα1 also interact at the NF-κB element of the *FOXM1* promoter. FOXM1 binds to the NF-κB element directly, whereas MATα1 requires the presence of either p50 or p65. Our previous finding that MAT1A inhibits NF-κB-driven promoter activity supports the notion that MATα1 also acts as a co-repressor of the NF-κB element. In contrast, FOXM1 positively regulates NF-κB in liver cancer mainly by suppressing *MAT1A* transcription and displacing MATα1 from binding to the NF-κB site. This explains the finding that

FOXM1's effect on NF-κB is lost in liver cancer cells that do not express MAT1A. Taken together, in liver cancer either an increase in FOXM1 or a fall in MAT1A can provide the fuel to drive the feedforward loop to enhance cancer progression.

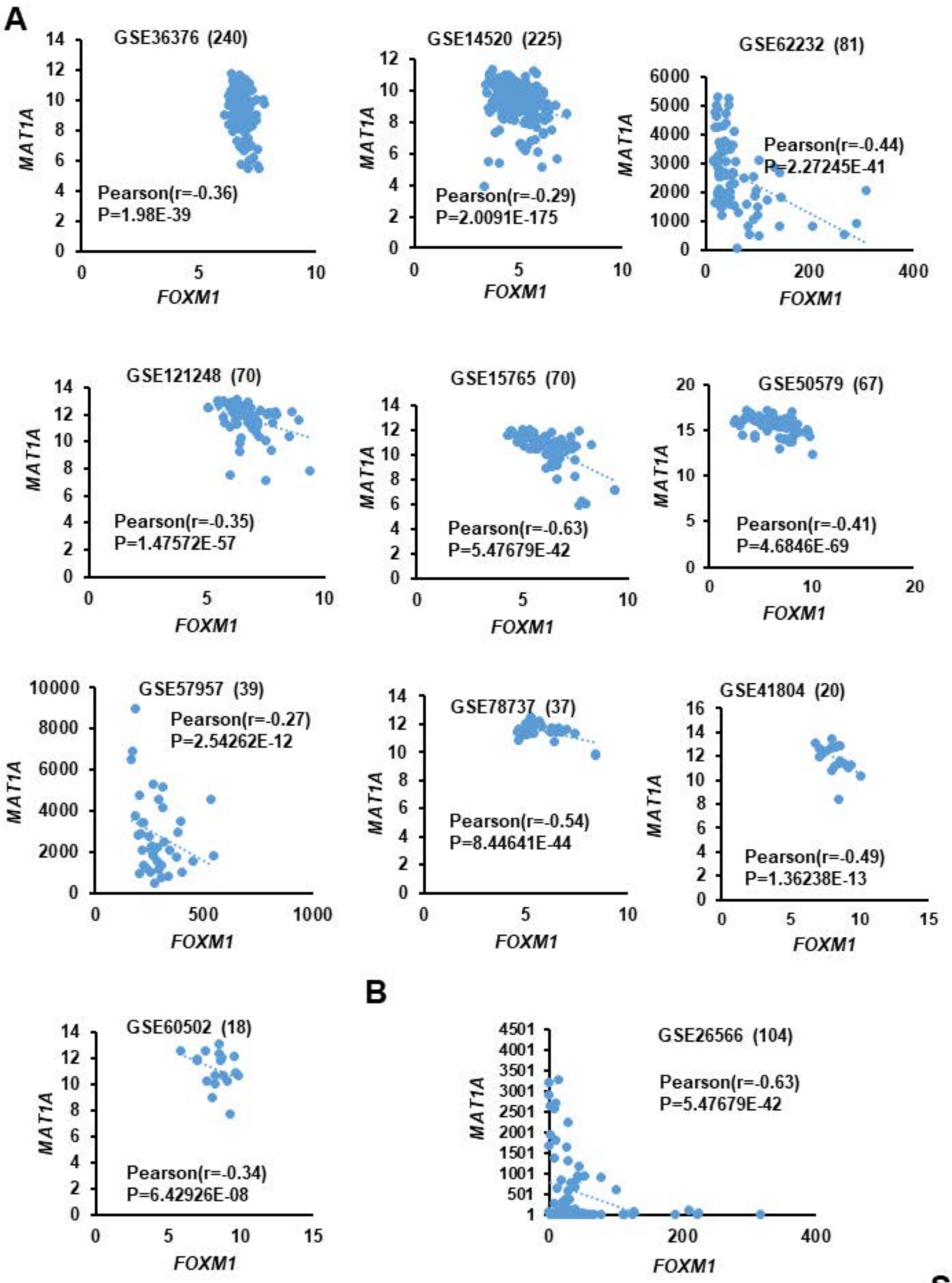
A
GSE36376 (240)
Pearson(r=-0.36)
P=1.98E-39
GSE14520 (225)
Pearson(r=-0.29)
P=2.0091E-175
GSE62232 (81)
Pearson(r=-0.44)
P=2.27245E-41
GSE121248 (70)
Pearson(r=-0.35)
P=1.47572E-57
GSE15765 (70)
Pearson(r=-0.63)
P=5.47679E-42
GSE50579 (67)
Pearson(r=-0.41)
P=4.6846E-69
GSE57957 (39)
Pearson(r=-0.27)
P=2.54262E-12
GSE78737 (37)
Pearson(r=-0.54)
P=8.44641E-44
GSE41804 (20)
Pearson(r=-0.49)
P=1.36238E-13
B
GSE60502 (18)
Pearson(r=-0.34)
P=6.42926E-08
GSE26566 (104)
Pearson(r=-0.63)
P=5.47679E-42
MAT1A
FOXM1

S1

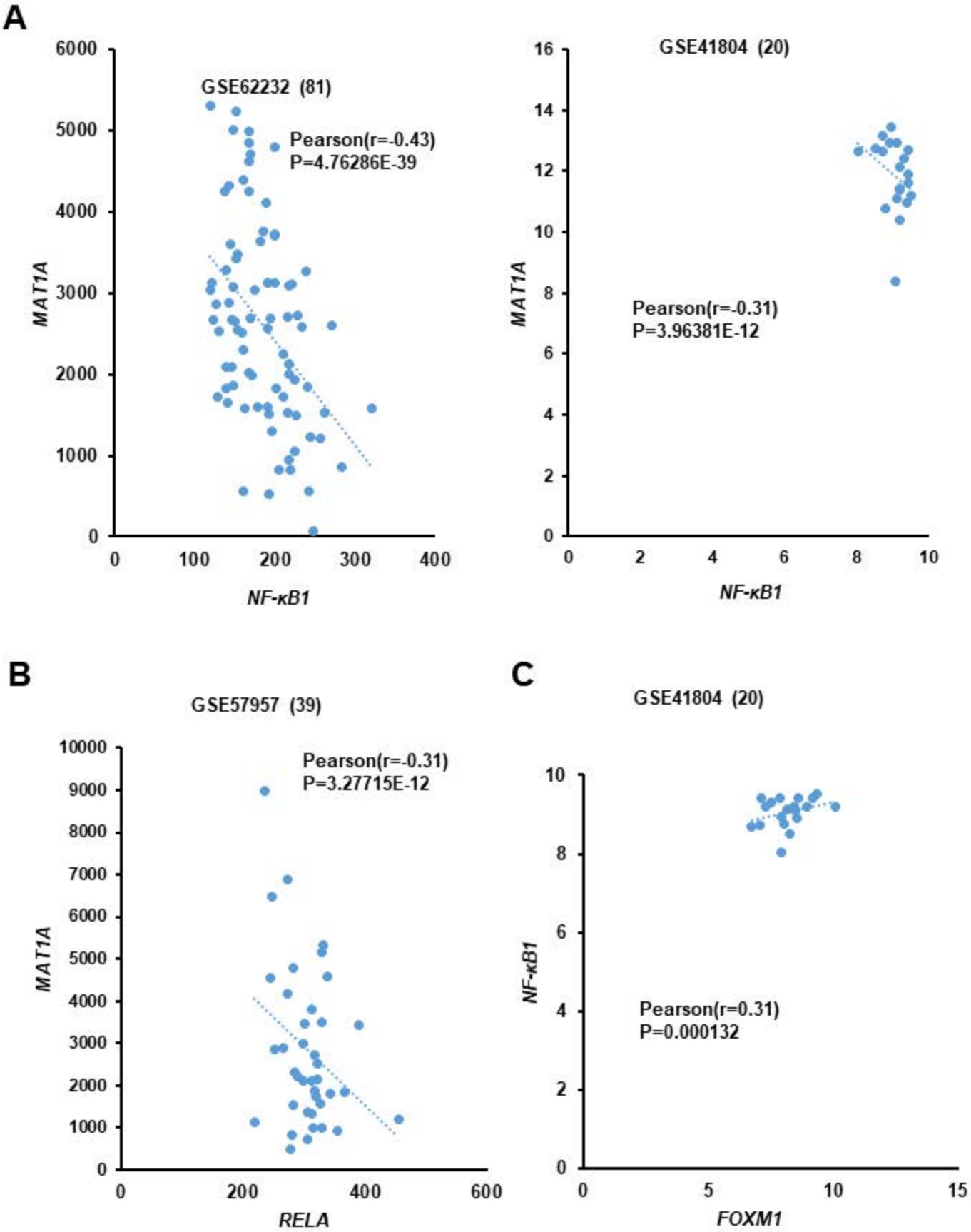
A
GSE62232 (81)
Pearson(r=-0.43)
P=4.76286E-39
MAT1A
NF-κB1
GSE41804 (20)
Pearson(r=-0.31)
P=3.96381E-12
MAT1A
NF-κB1
B
GSE57957 (39)
Pearson(r=-0.31)
P=3.27715E-12
MAT1A
RELA
C
GSE41804 (20)
Pearson(r=0.31)
P=0.000132
NF-κB1
FOXM1

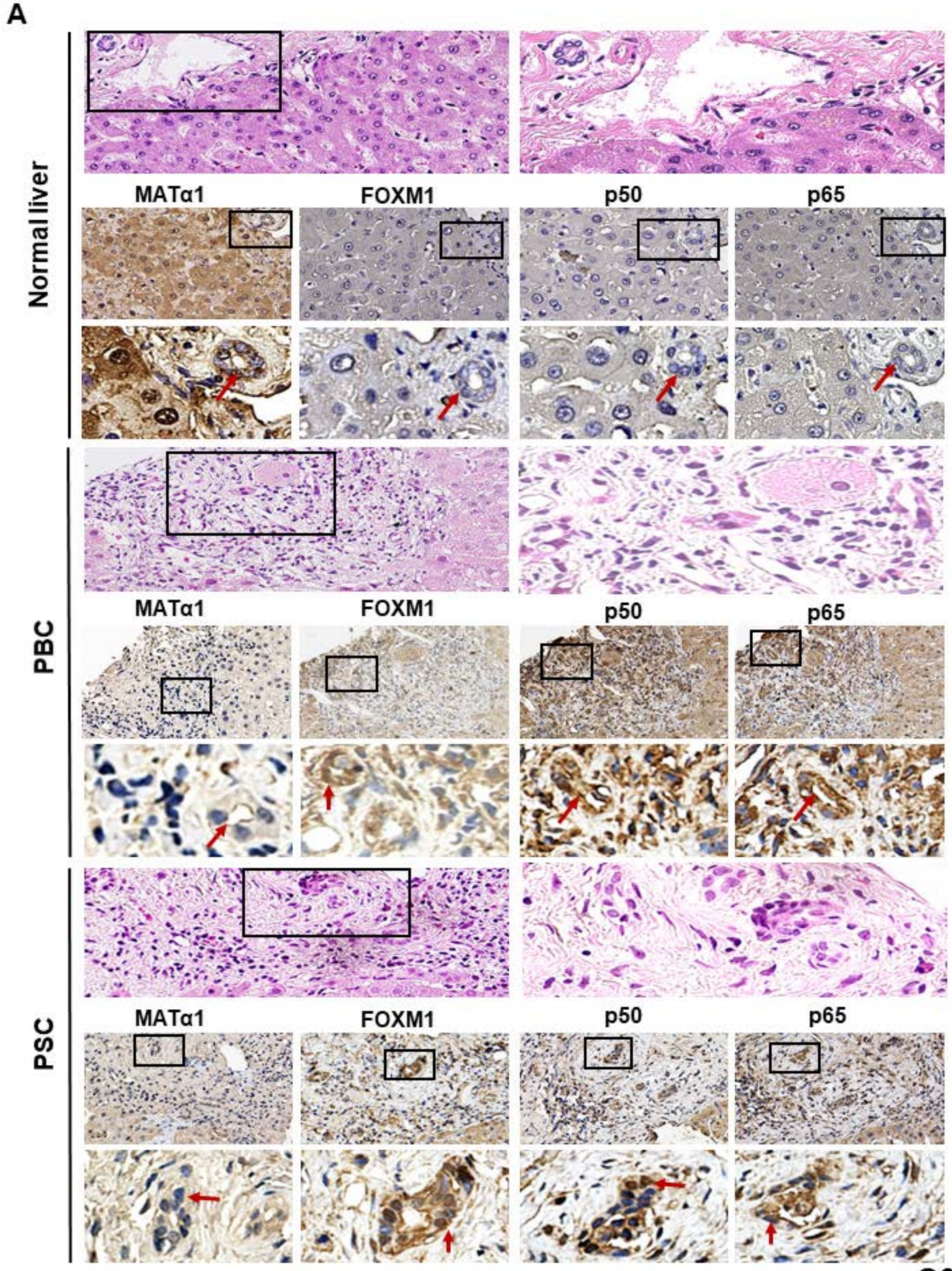
A
Normal liver
MATα1
FOXM1
p50
p65
PBC
MATα1
FOXM1
p50
p65
PSC
MATα1
FOXM1
p50
p65

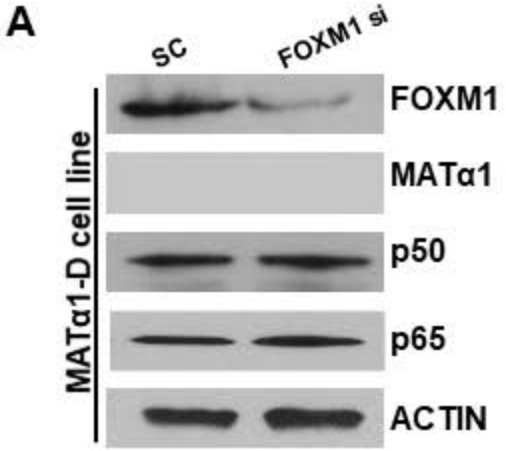
A
SC
FOXM1 si
MATα1-D cell line
FOXM1
MATα1
p50
p65
ACTIN

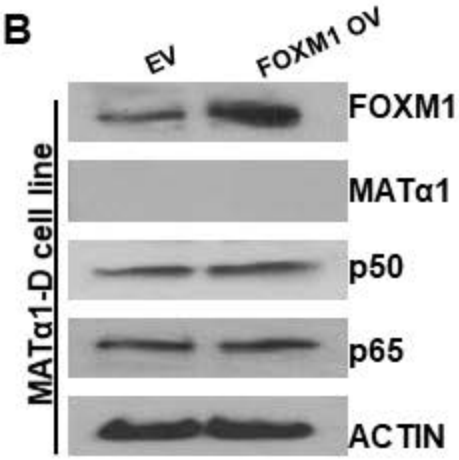
B
EV
FOXM1 OV
MATα1-D cell line
FOXM1
MATα1
p50
p65
ACTIN

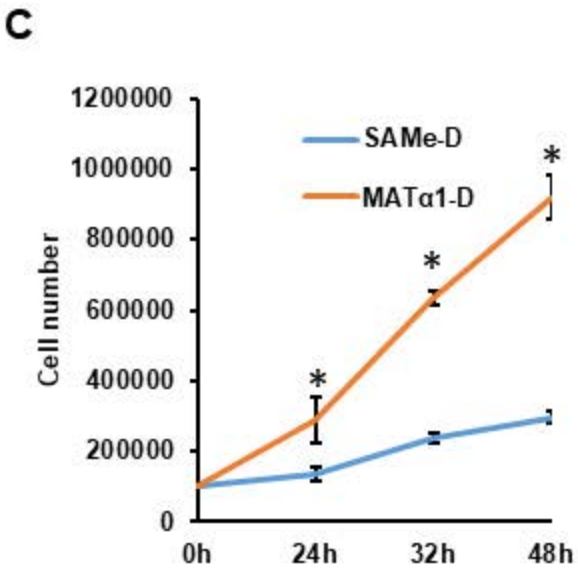
C
Cell number
1200000
1000000
800000
600000
400000
200000
0
SAMe-D
MATα1-D
0h
24h
32h
48h

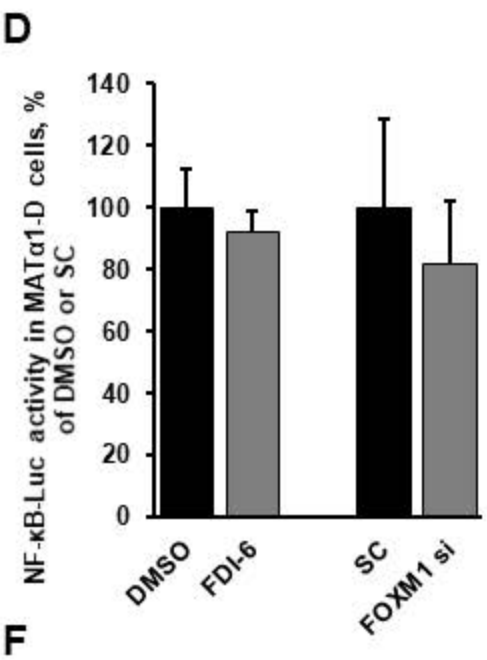
D
NF-κB-Luc activity in MATα1-D cells, % of DMSO or SC
140
120
100
80
60
40
20
0
DMSO
FDI-6
SC
FOXM1 si

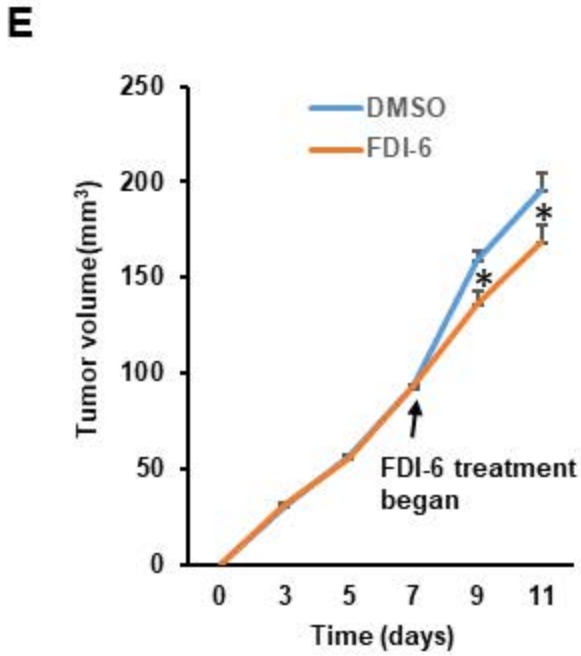
E
Tumor volume(mm³)
250
200
150
100
50
0
DMSO
FDI-6
FDI-6 treatment began
0
3
5
7
9
11
Time (days)

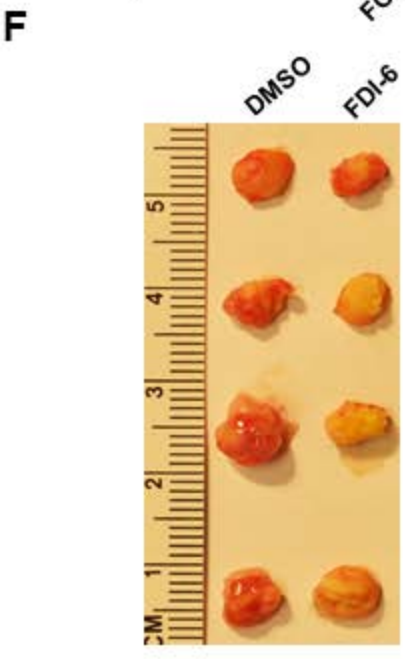
F
DMSO
FDI-6

A

***MAT1A* promoter**

-1111 AATG TGTGCCAGAA
-1097 AAAATTTTTC CAAATGCTTG ATAATAAACT CAGAGGGGGG TTTGGTCACC AGAATTGTTA
C/EBP AP1
-1037 GGTGAGGCTA TTGCTTCCTA ACTTTTGCTT CCCACAGTCC AAGCTTTGAT GCACAAGGTT
-977 ATGGTTGATT ACTTTTTATT GCATTCTAGT GGGAACTGGT TTCTCCACCC ATCCTCATTT
-917 TCTGTGGTCT CAATTCCCCA TTGTTCCTTG GGTCTGAGGA TGCAGCTGGA TCTGAGAGTG
-857 TGAGACGCTG TCATTTAGTA CATGAACTAA AGATATAATC CTGTTTACTA CTTTTTTTGG
FOX
-797 TCAAAGCAAA AAATAATGCA AGAGTTATGT GAACACGATG TTTATTACAT GTATAGAACT
FOX
-737 GAATATGTAG ATGTTTATAA TCCGGAAGCT TTGGGAAACT GGACTTTGAT AATTTCCCTG
FOX C/EBP
-677 TAATGAATCC ATTTCTCAAA AGCATTTTTT TCTAAAAAAA ACACACACAC ACACACACAC

-617 ACACACACAT TGTTCTCTGT AACCTCCCCA GATAGATACT TTTTAAAGAT CTTGCTTGTT

-557 AAAATGCCTG CCAGCCTTTT AGAGAAGTTG ACAGGTTAGG TGGTTTCTGT TAGCAGAAAC
-497 ACGTGGACTC AAAGCTTTTC CTCTAAAATG AATCTGTTGT GTAACATCAC AGCTGGCTCA
E-Box
-437 GAATACAGGT GCGTGCTCCT GCTCTCCCTG AGAAGATAGA ATGGGAAGAG ACCAATCCAG
-377 ATGAGACGCA GGGGAGGAGG GGACACCCAA CAGCAAAGGC ACTGTTGCAA TCTTAGCCTA
C/EBP
-317 AACCATATCT CTGAGAAAGA GTTTCTTGTT GCCTGCTTGT ATCTCTGGGT GATCACAGAC
-257 CCCTGCTCTC CAAGGTGGGT TGTGAACTCT GGAGCACTAC CAAGATTGGC TAAGAGCTGA
-197 AGGAGAGTCC CAAAGGAGCT TCAATTCTGC AGAACTATAC AGCCTTCTTT ACCTTACCTT
-137 GACCAGGTGC TTAGAGTTTGGAAAGTCAGG GATAAGAATT GAAATTCCTC CAGGTAAGAA
C/EBP
-77 GACCCCCCTC TTAGGAAATG GACTCCTCCA ATTTTCTCAC ATGATTTTTC AGGCACTTTC
-17 GCTTTTCCAT ATATAGG
C/EBP TATA Box TSS

B

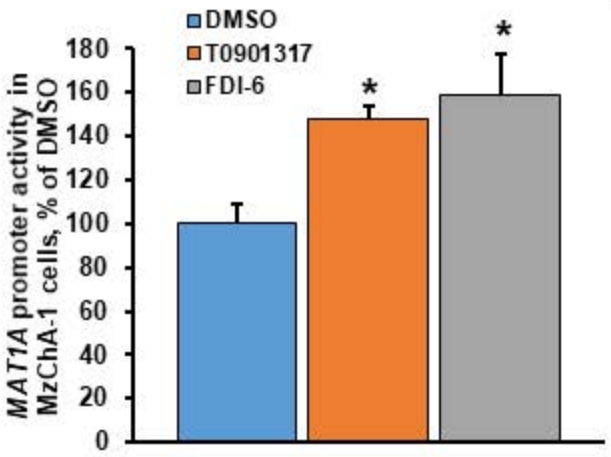

C

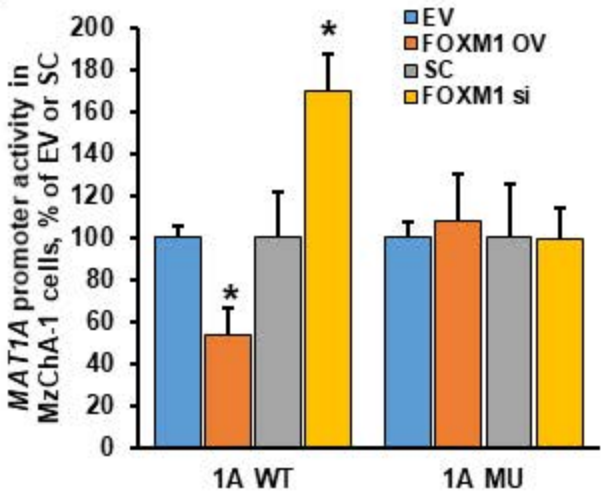

A

***FOXM1* promoter**

```
-1304                                  AA CTCACACCAC ACTCCATTCA GGTCGATTAG
-1272 CTCAAACCCC TCAGATATTT CTCAGCCTTT GTACTCACTG TGCTTCCTCC TGCCATCCAG
-1212 CCTTTGCACG CCTGATTCCC TCTGCTTAGA GGAGTTCCCT CCTTTCTTTG TAAAAGGCAT

-1152 CAGATCTCAC ACCAAGCTCT CATTACAAAA GCCTTTCCTG TCCTACCTCT CAAGATCTCG
-1092 TTATTGTAAA TACTCAAAGT ATCATTAACC TCTAATGTTT CAATTTACAG CAATAATTCA
-1032 ACATTTGTTT GTTTTGGAGA CGGTGTCTCC CTCTGTCGCC CAGGCTGGAG TGCAGTGGTG
           FOX      NF-κB
-972  TGATCATGGC TTACCATAGC CTCCACCTCT CGGCCTCAGG TGATCCTTCC ACCTCAGCCT
-912  CCAGAGTAGC TGGGACTACA GGCACGCACC ACCACGCCCG GCTAATTTTT AGTAGAGAAG
-852  CGGTTTCGCT ATGTTGCCAG GCTGGTCTCG AACTCGTGAC CTCAAGTGAT CCACCCGCCT
-792  CGGCCTCCTA AAGTGCTGGG ATTACAGGCG TGAGCCACTA TGCCCAGCCC ACATTTGTTT
                                                                    FOX
-732  ATTTGATTAA AATGTCTGTG CCCCTCTTCC AGGATTGGGC TGTGAGCCCA GGGGAAGGAA

-672  AGAACCTTGT CTGCCATTGT ATCTTCAGGG CCTAGCGGTG CCTGGCGCAC AGCAGTTGCT
      NF-κB
-612  CAACTAGACT GGTTGACTAA GTCAATAAAT AAAGCACTAC GGTCTATTAT ATCCGAAGGC
-552  TTGGCTTCGG GAGGGGCAAA AGACAGGTTT CGCGCTGAGG TAGGGTTCAT GGTGCCGACA
-492  TTTTTTTTCA AGATGGAAGA AAGCGGAGAT AATACGCAGC CCTCAAAGGA ACTTAGTCTA
-432  ATCGGGGGGA GCAGACGATC GTTCACTGTG GGAAAATGGG GTACGATTTC CCCCAGTGAG
-372  GAAATCAACT AAAGCCGAGC TTTGAAAAGG GGAGCAGAGG AGCCTGAGGG GAAGCGGGGG
-312  CGTGTCGCCT GGCGTGACCA GCGCGGCAGG AAAAGCGGGC CCAGGGACCC GGGCCTGTCA
-252  CGCCGCTTCC GCGCGTCCCC AAACTCTCCC TCGGCTCGCC CACCCACGCG GCGGGGACCC
-192  CTCCGGCCCC TCCCCGGCCC CACGGCCACT TCTTCCCCCA CAAGCCGGCC TGCGGTCCGC
-132  CTTACCAGCC CGGGCCGGAC GGGGCCGCAG CTCCTGGCAG ACCGCACAGC CTTCGAGCCC
-72   GGAATGCCGA GACAAGGCCG GCGCCGATTG GCGACGTTCC GTCACGTGAC CTTAACGCTC
-12   CGCCGGCGCC AAT                  NF-κB       E-Box
```

B

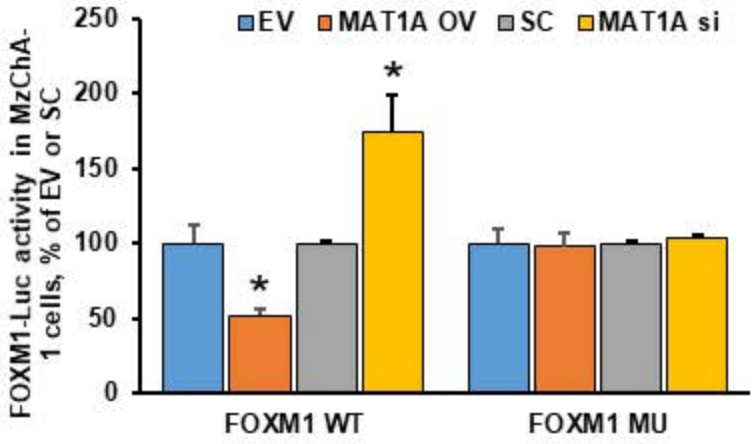

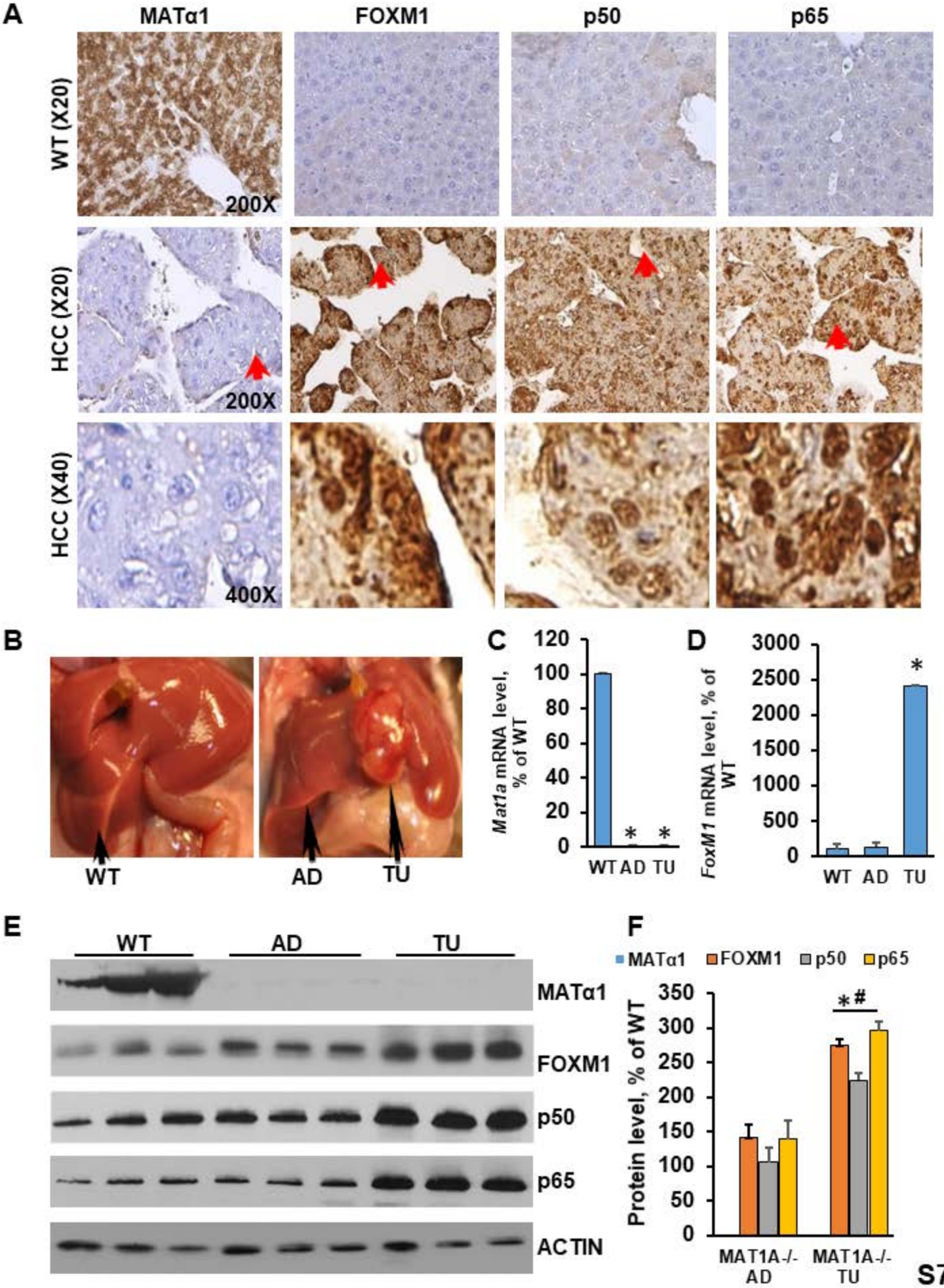
A
MATα1
FOXM1
p50
p65
WT (X20)
200X
HCC (X20)
200X
HCC (X40)
400X
B
WT
AD
TU
C
Mat1a mRNA level, % of WT
120
100
80
60
40
20
0
*
*
WT AD TU
D
FoxM1 mRNA level, % of WT
3000
2500
2000
1500
1000
500
0
*
WT AD TU
E
WT
AD
TU
MATα1
FOXM1
p50
p65
ACTIN
F
MATα1
FOXM1
p50
p65
Protein level, % of WT
350
300
250
200
150
100
50
0
*#
MAT1A-/- AD
MAT1A-/- TU

S7

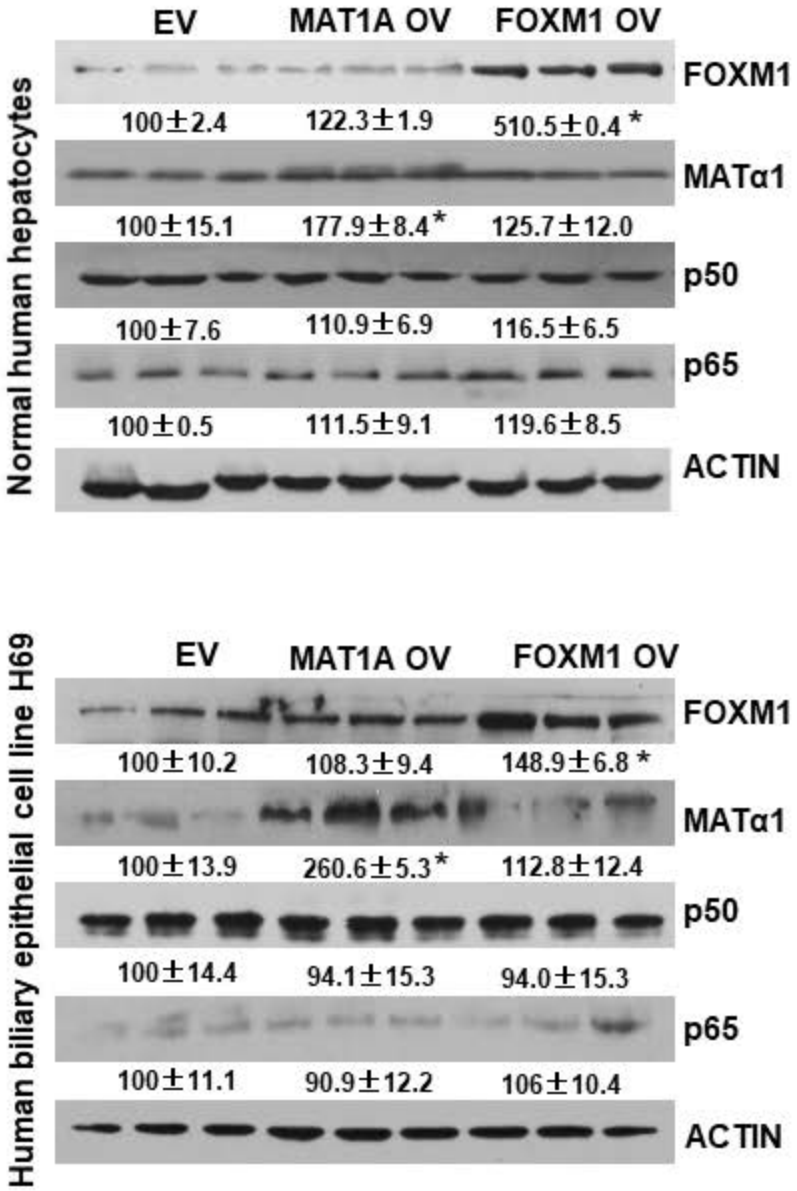
EV
MAT1A OV
FOXM1 OV
Normal human hepatocytes
FOXM1
100±2.4
122.3±1.9
510.5±0.4 *
MATα1
100±15.1
177.9±8.4*
125.7±12.0
p50
100±7.6
110.9±6.9
116.5±6.5
p65
100±0.5
111.5±9.1
119.6±8.5
ACTIN
EV
MAT1A OV
FOXM1 OV
Human biliary epithelial cell line H69
FOXM1
100±10.2
108.3±9.4
148.9±6.8 *
MATα1
100±13.9
260.6±5.3*
112.8±12.4
p50
100±14.4
94.1±15.3
94.0±15.3
p65
100±11.1
90.9±12.2
106±10.4
ACTIN

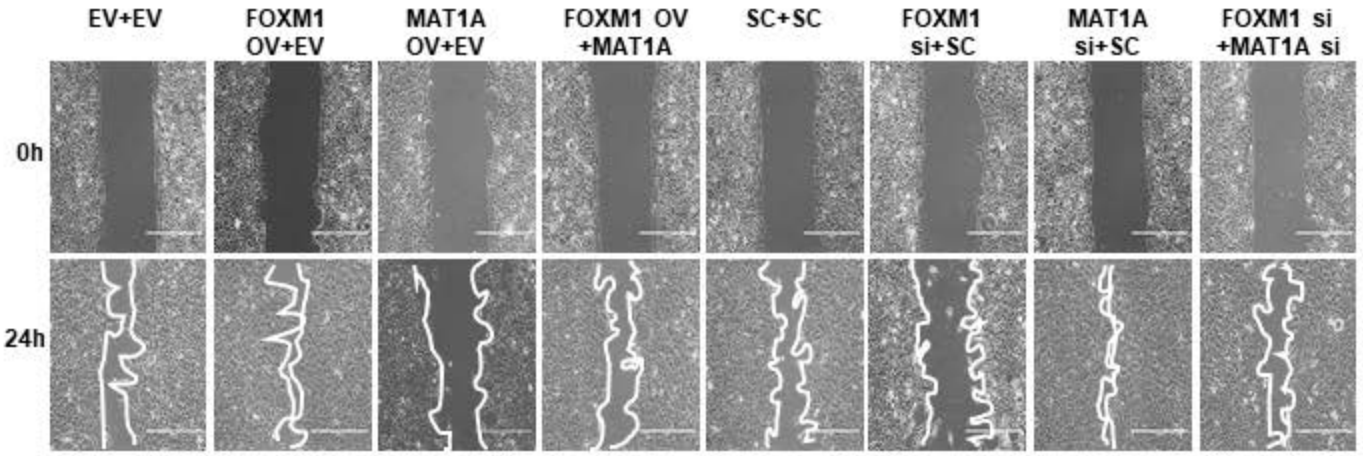
EV+EV
FOXM1 OV+EV
MAT1A OV+EV
FOXM1 OV +MAT1A
SC+SC
FOXM1 si+SC
MAT1A si+SC
FOXM1 si +MAT1A si
0h
24h

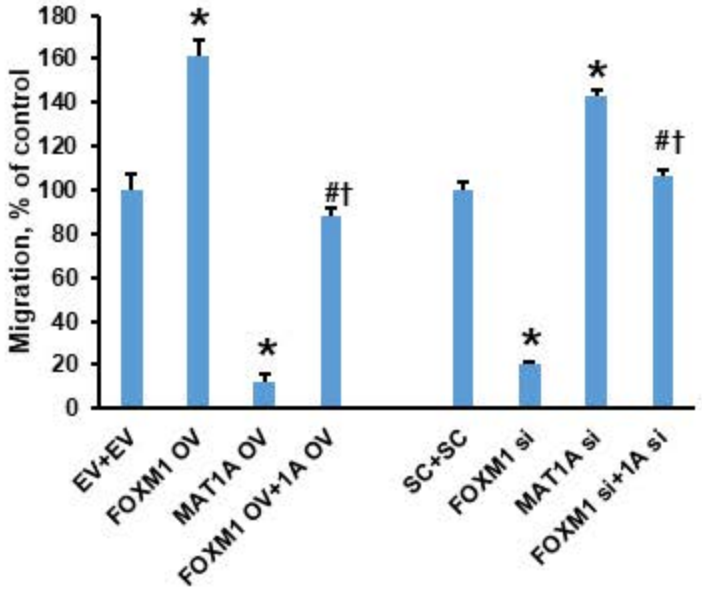
Migration, % of control
180
160
140
120
100
80
60
40
20
0
*
*
*
*
#†
#†
EV+EV
FOXM1 OV
MAT1A OV
FOXM1 OV+1A OV
SC+SC
FOXM1 si
MAT1A si
FOXM1 si+1A si

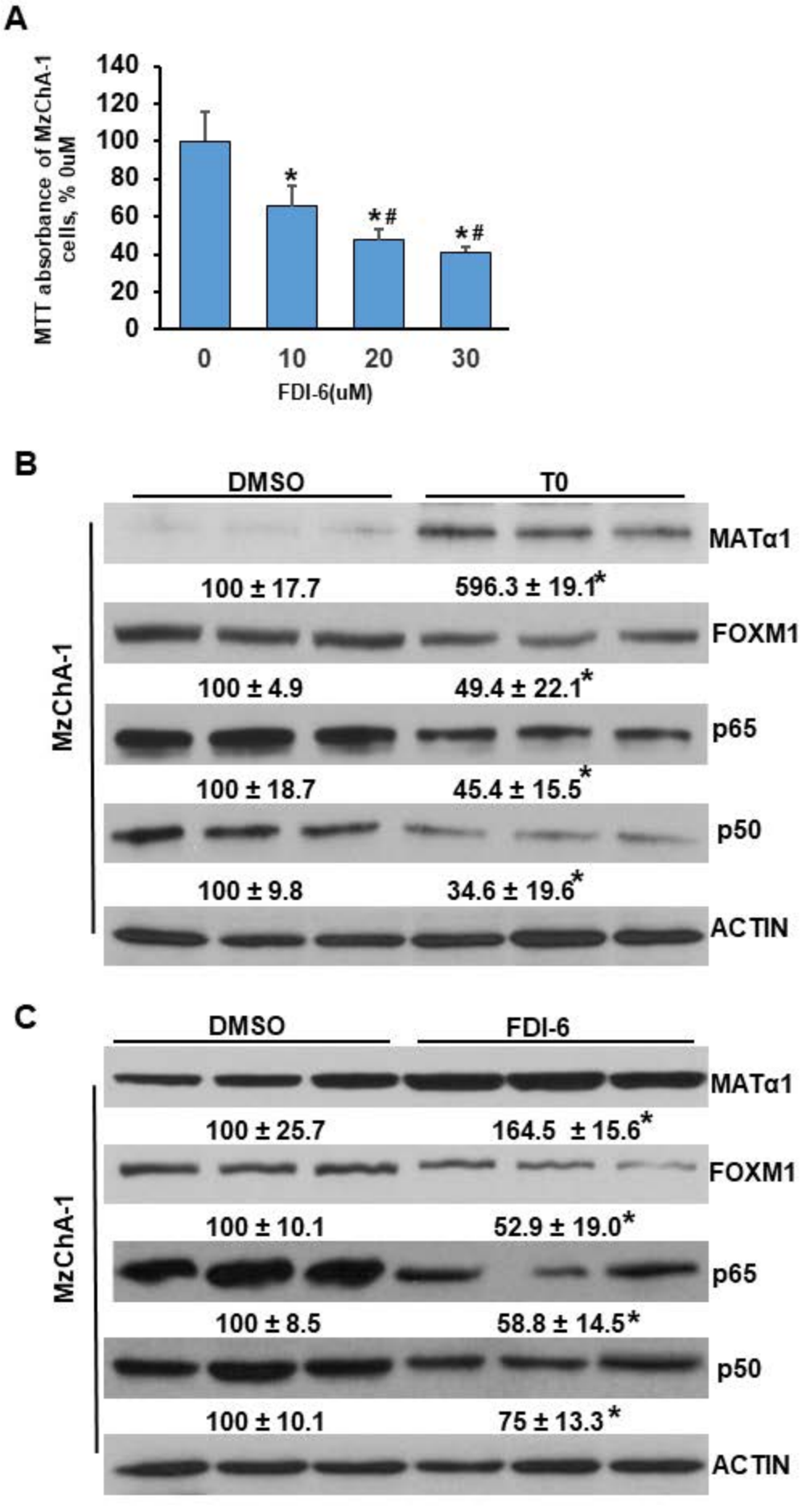
A
MTT absorbance of MzChA-1 cells, % 0uM
140
120
100
80
60
40
20
0
*
*#
*#
0
10
20
30
FDI-6(uM)
B
DMSO
T0
MzChA-1
MATα1
100 ± 17.7
596.3 ± 19.1*
FOXM1
100 ± 4.9
49.4 ± 22.1*
p65
100 ± 18.7
45.4 ± 15.5*
p50
100 ± 9.8
34.6 ± 19.6*
ACTIN
C
DMSO
FDI-6
MzChA-1
MATα1
100 ± 25.7
164.5 ± 15.6*
FOXM1
100 ± 10.1
52.9 ± 19.0*
p65
100 ± 8.5
58.8 ± 14.5*
p50
100 ± 10.1
75 ± 13.3*
ACTIN

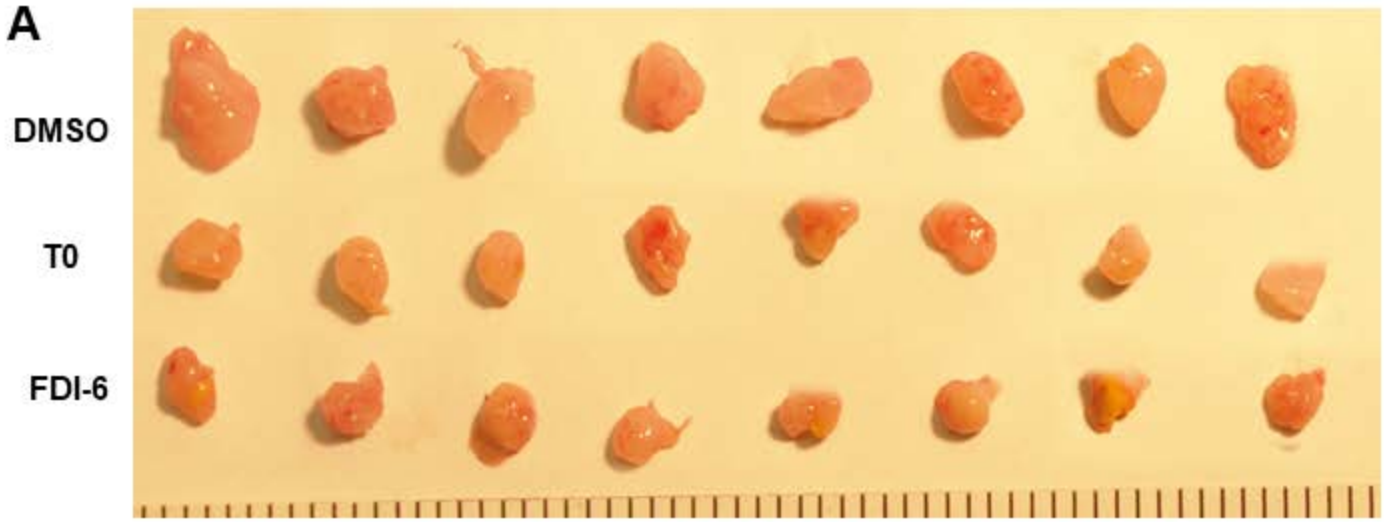
A
DMSO
T0
FDI-6

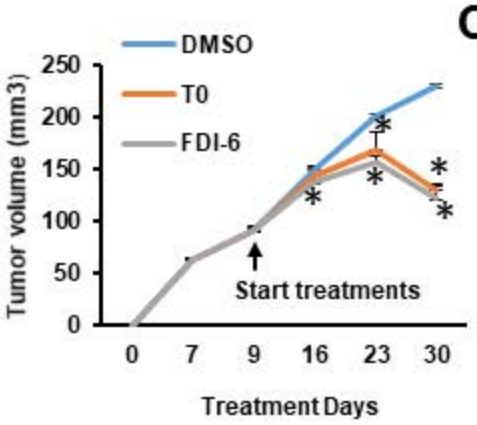
B
DMSO
T0
FDI-6
Tumor volume (mm3)
250
200
150
100
50
0
Start treatments
0
7
9
16
23
30
Treatment Days

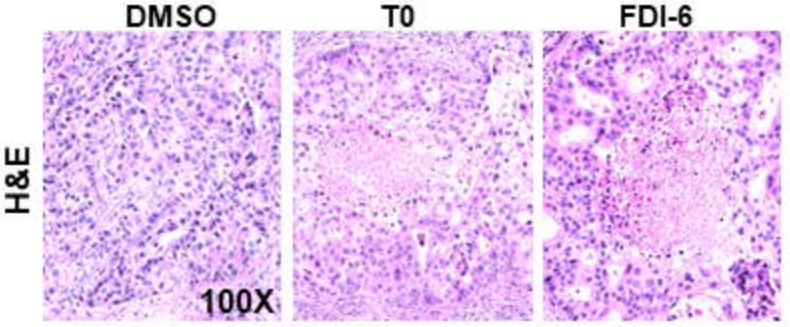
C
DMSO
T0
FDI-6
H&E
100X

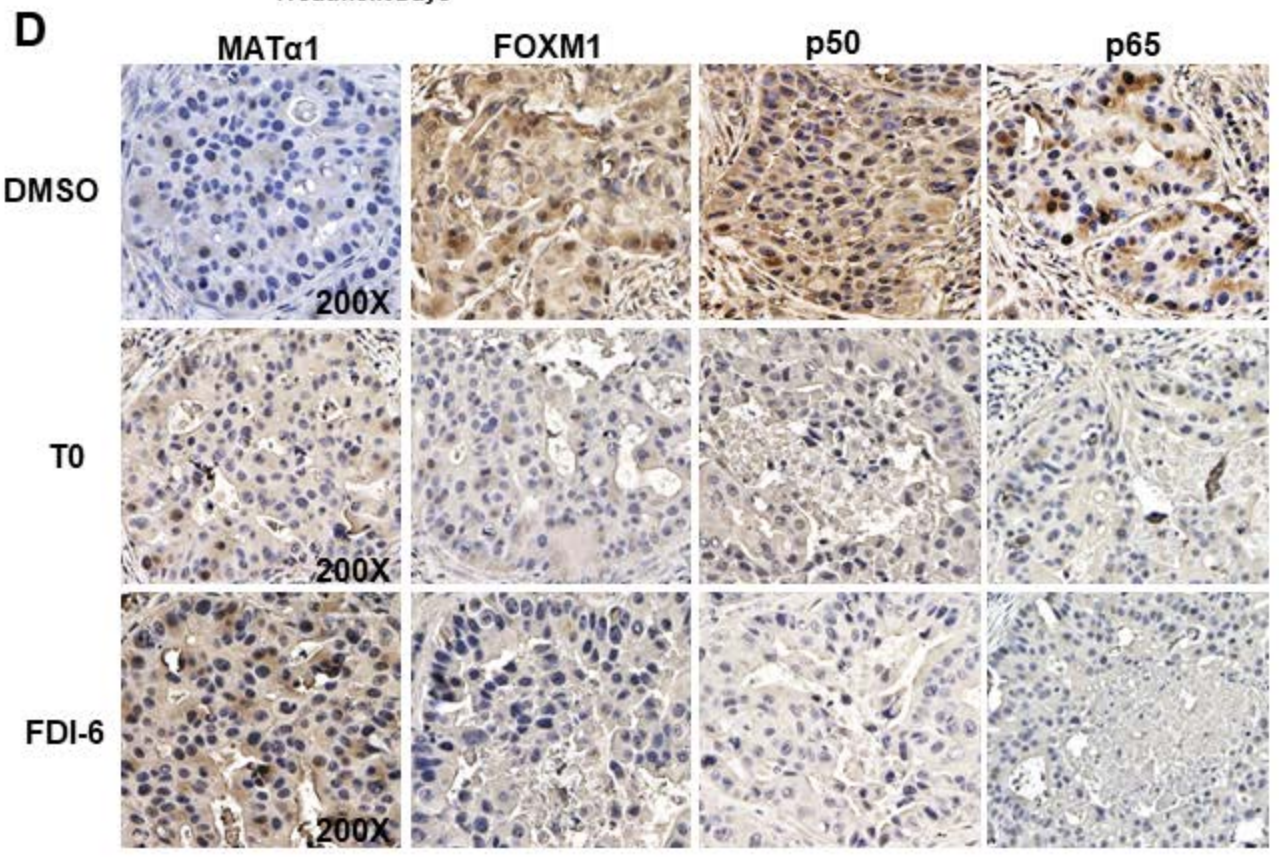
D
MATα1
FOXM1
p50
p65
DMSO
T0
FDI-6
200X
200X
200X

A Ingenuity pathway of MAT1A, NF-kB and FOXM1 in CCA

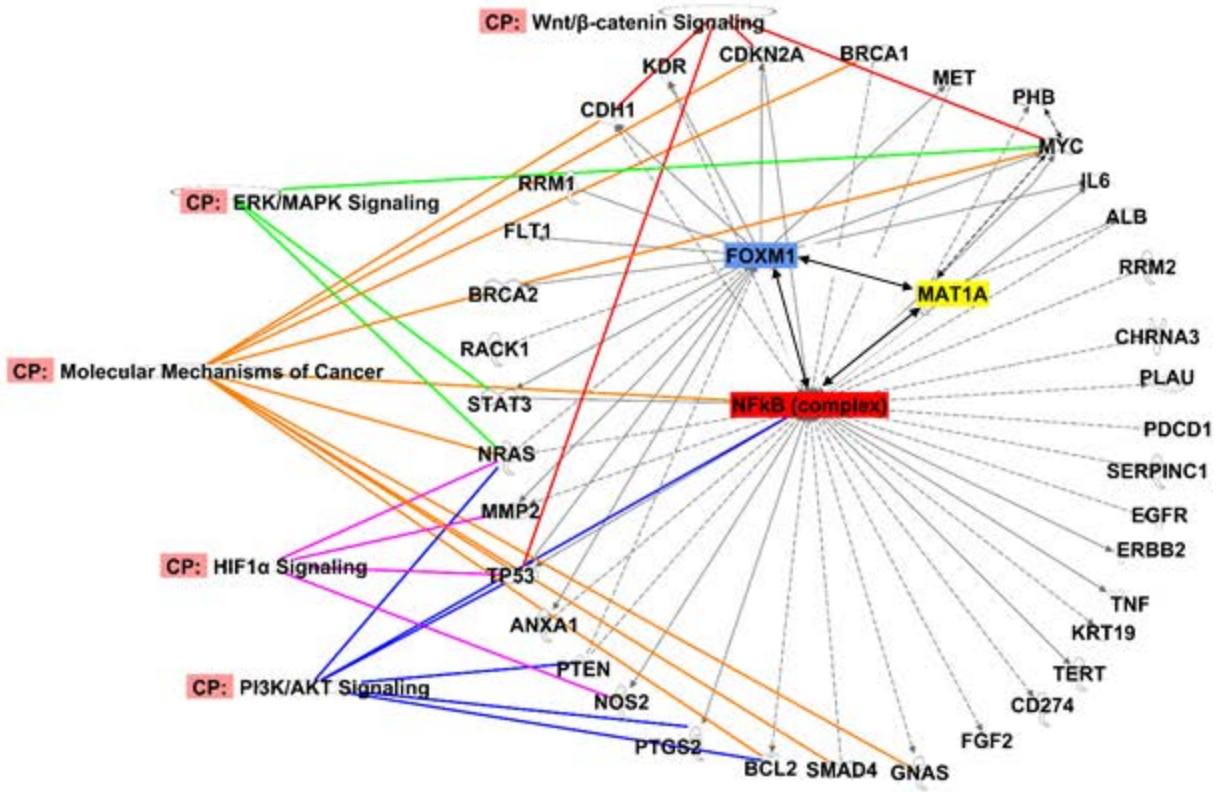

B Ingenuity pathway of MAT1A, NF-kB and FOXM1 in HCC

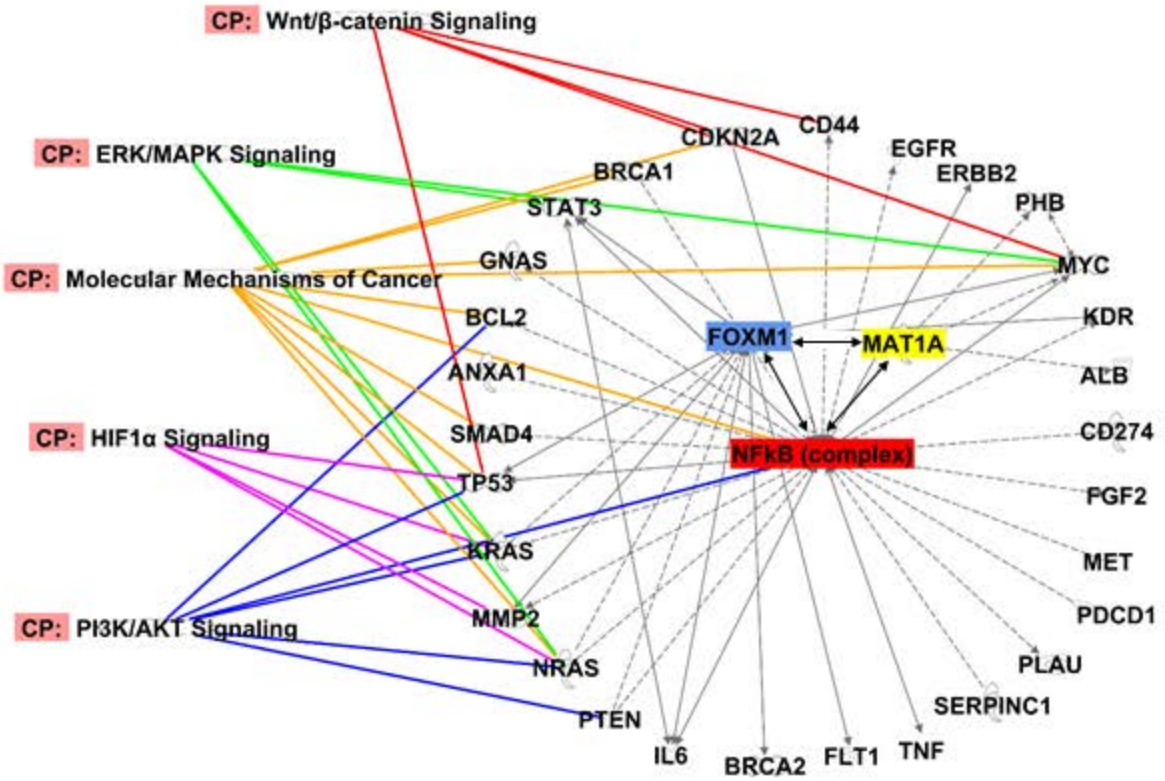

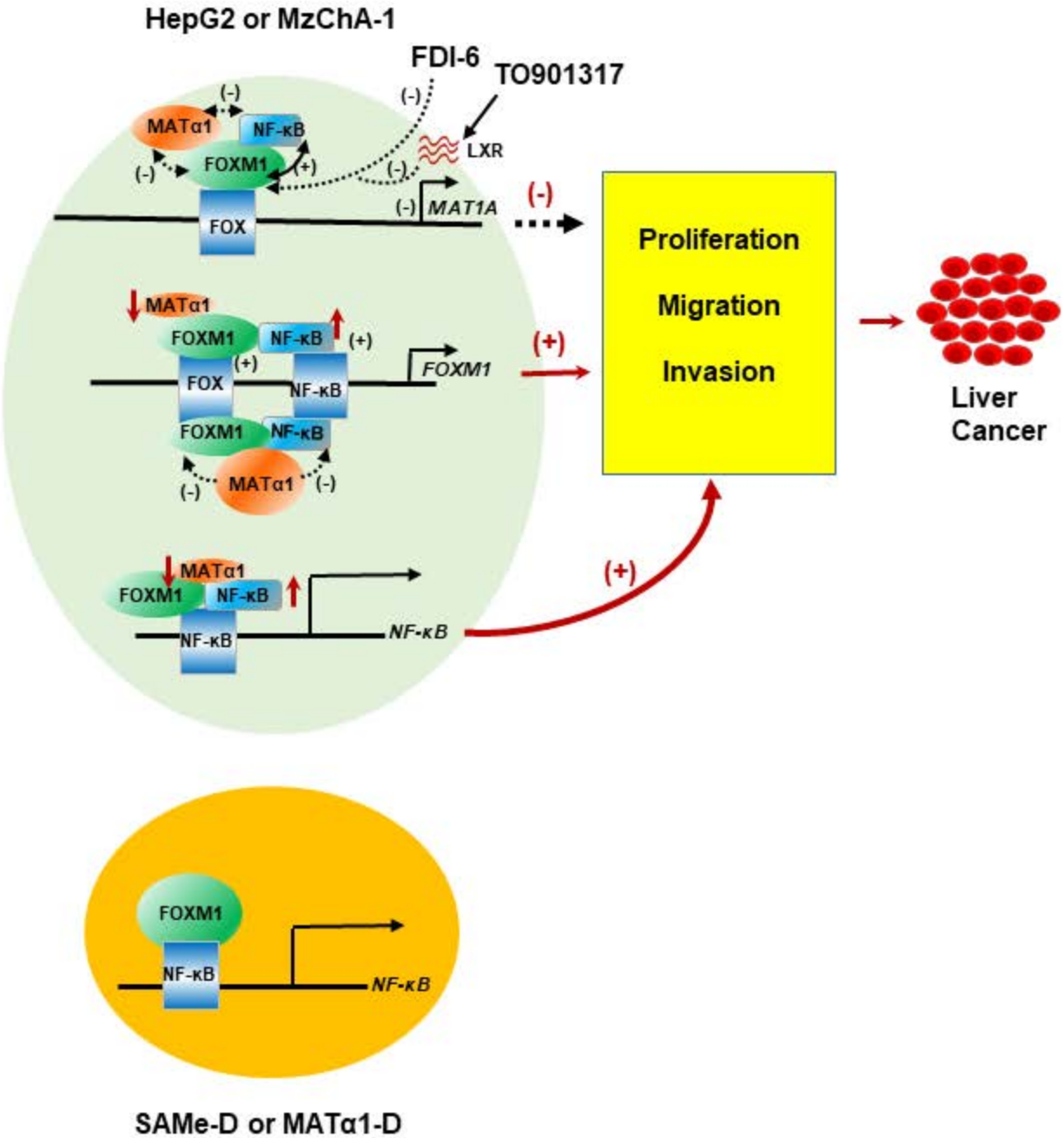
HepG2 or MzChA-1
FDI-6
TO901317
LXR
MATα1
NF-κB
FOXM1
FOX
MAT1A
(-)
(+)
Proliferation
Migration
Invasion
Liver Cancer
FOXM1
NF-κB
SAMe-D or MATα1-D

Supplemental Table 1. Fold changes of *MAT1A* and *FOXM1* mRNA levels in datasets

Datasets	Type of live cancer	Fold change of mRNA	
		MAT1A	*FOXM1*
GSE50579	Human patients with genetic hemochromatosis	-1.77	2.44
	Human patients with HBV infection	-1.98	13.4
	Human HCC patients	-2.51	11.9
	Human patients with HCV infection	-1.99	13.0
	Human patients with cryptogenic (unknown)	-2.98	9.17
GSE6222	Human liver cancer cell line (Huh7)	-38.4	22.6
	Human HCC stage T3	-5.51	6.07
GSE54238	Human HCC advanced stage	-4.81	6.0
GSE25097	Human HCC patient	-1.94	6.5
GSE29721	Human HCC patient	-2.95	3.89
GSE33294	Human HCC samples from China	-7.85	19.6
GSE55092	LCM Hepatocytes of HCC patients with HBV	-2.35	3.92
	Liver biopsies of HCC patients tumor -center with HBV	-4.91	3.83
	Liver biopsies of HCC patients tumor -periphery with HBV	-2.6	3.08
GSE12443	Human HCC patient	-2.24	1.41
GSE1898	MYC-driven liver cancers in a musculus model	-9.24	6.2
GSE6764	Human HCC patients very advanced	-3.77	3.86
	Human HCC patients advanced	-2.03	2.12
	Human HCC patients very early	-1.56	1.41
GSE94660	Human HCC patients HBV	-4.78	9.65
TCGA	Human HCC patients from TCGA	-3.55	14.47
GSE62232	Human HCC patients	-3.19	2.62
GSE36411	Undifferentiated HCC Grade III-IV	-3.2	2.97
	Differentiated HCC Grade III-IV	-6.56	2.11
	Differentiated HCC Grade I-II	-2.4	1.5
GSE60502	Human HCC patients	-3.05	2.34
GSE14520	Human HCC patients vs. livers of healthy donors_GPL571	-3.08	3.19
	vs. non-tumor liver tissues_GPL5	-4.58	2.78
	vs. non-tumor liver tissues_GPL3921	-3.61	2.16
GSE5364	Human HCC patients	-110	9.98
GSE55758	Human HCC patients	-3.14	2.64
GSE57957	Human HCC patients	-2.76	1.47
GSE22405	Human HCC patients	-2.1	1.55
GSE39791	Male HCC patients	-2.01	1.7
GSE104766	Proliferative hepatoblastoma patients	-7.46	1.77
E-MEXP-1851	Hepatoblastoma tumor	-3.42	1.41
GES36376	Human HCC patients	-2.52	1.44
GSE26566	Human CCA patients vs. non-cancerous surrounding	-40.5	9.53
	Human CCA patients vs. intrahepatic bile duct	-18.4	11.7

Fold changes are relative to adjacent non-tumorous or normal liver tissues

Supplemental Table 2. Fold changes of *RELA and FOXM1* mRNA levels in datasets

Datasets	Type of liver cancer	Fold change of mRNA	
		RELA	***FOXM1***
GSE19665	Human patients with HBV infection	1.42	3.21
GSE6764	Human HCC patients very early	1.26	1.41
	Human HCC patients	2.48	9.98
	Human HCC patients advanced	1.32	2.1
	Human HCC patients very advanced	1.38	3.86
GSE55092	LCM Hepatocytes of HCC patients with HBV	1.42	3.92
GSE29721	Human HCC patients	1.3	3.89
GSE40367	Human HCC patients with lung metastases	1.43	5.73
E-MEXP-1851	Hepatoblastoma tumor	1.3	1.41
GSE39791	Male HCC patients	1.21	1.39
	Human HCC patients	1.2	1.44

Fold changes are relative to adjacent non-tumorous or normal liver tissues

Supplemental Table 3. Fold changes of *NF-κB1* and *FOXM1* mRNA levels in HCC datasets

Datasets	Type of liver cancer	Fold change of mRNA	
		NF-κB1	***FOXM1***
GSE39791	Male HCC patients	1.68	1.39
	Human HCC patients	1.64	1.44
GSE36376	Human HCC patients	1.33	1.44

Fold changes are relative to adjacent non-tumorous or normal liver tissues